Published online 9 September 2011 *Nucleic Acids Research, 2012, Vol. 40, No. 1* ***461–475***
doi:10.1093/nar/gkr670

The insertion of two 8-methyl-2′-deoxyguanosine residues in tetramolecular quadruplex structures: trying to orientate the strands

Antonella Virgilio[1], Veronica Esposito[1], Giuseppe Citarella[1], Antonietta Pepe[2], Luciano Mayol[1] and Aldo Galeone[1,*]

[1]Dipartimento di Chimica delle Sostanze Naturali, Università degli Studi di Napoli 'Federico II', Via D. Montesano 49, I-80131 Napoli and [2]Dipartimento di Chimica ''A. M. Tamburro'', Università degli Studi della Basilicata, Viale dell'Ateneo Lucano 10, I-85100 Potenza, Italy

Received July 14, 2011; Revised July 28, 2011; Accepted July 29, 2011

ABSTRACT

In this article, we report a structural study, based on NMR and CD spectroscopies, and molecular modelling of all possible d(TG_3T) and d(TG_4T) analogues containing two 8-methyl-2′-deoxyguanosine residues (M). Particularly, the potential ability of these modified residues to orientate the strands and then to affect the folding topology of tetramolecular quadruplex structures has been investigated. Oligodeoxynucleotides (ODNs) TMMGT (T12) and TMMGGT (F12) form parallel tetramolecular quadruplexes, characterized by an all-*syn* M-tetrad at the 5′-side stacked to all-*anti* M- and G-tetrads. ODNs TMGMT (T13) and TMGGMT (F14) form parallel tetramolecular quadruplexes, in which an all-*anti* G core is sandwiched between two all-*syn* M-tetrads at the 5′- and the 3′-side. Notably, the quadruplex formed by T13 corresponds to an unprecedented structure in which the *syn* residues exceed in number the *anti* ones. Conversely, ODN TGMGMT (F24) adopts a parallel arrangement in which all-*anti* G-tetrads alternate with all-*syn* M-tetrads. Most importantly, all data strongly suggest that ODN TMGMGT (F13) forms an unprecedented anti-parallel tetramolecular quadruplex in which G and M residues adopt *anti* and *syn* glycosidic conformations, respectively. This article opens up new understandings and perspectives about the intricate relationship between the quadruplex strands orientation and the glycosidic conformation of the residues.

INTRODUCTION

Nucleic acid quadruplexes are DNA and RNA secondary structures based on a planar arrangement of four guanines, called G-tetrad or G-quartet, which can be considered as their structural unit. The remarkable stability of these structures is one of their most important characteristic and, probably the reason of their large spread in several significant genomic regions (1). Apart the natural occurrence of these structures (promoter region, centromeres, telomeres, etc.), quadruplexes can also be adopted by a number of aptamers endowed by noteworthy biological activities including anti-HIV (2 and references cited therein), anti-proliferative (3 and references cited therein) and anti-coagulation aptamers (4,5 and references cited therein). Furthermore, several deoxyribozymes have been found to contain quadruplexes as structural elements (6). In addition, quadruplex structures seem to be involved in some genetic human diseases (7). A characteristic feature of G-quadruplexes is their dramatic structural variability involving several aspects mutually interconnected as the molecularity, the relative strands arrangement, the glycosidic conformation of the residues (*syn* or *anti*), the size of the grooves and the presence of loops connecting the strands (8).

In view of the biological relevance of these structures, the understanding of the molecular forces that rule the quadruplex folding is of particular interest. As a matter of fact, a number of reports have identified several factors that are able to affect the quadruplex structures folding topology: (i) the number of G-tetrads that can form: folding topologies should be preferred characterized by a higher quantity of stacked G-tetrads; (ii) the strand concentration: higher concentration should favour the formation of complexes with higher molecularity; (iii) the length

*To whom correspondence should be addressed. Tel: +39 081 678542; Fax: +39 081 678552; Email: galeone@unina.it

The authors wish it to be known that, in their opinion, the first two authors should be regarded as joint First Authors.

and the base composition of the loops (9–12); (iv) the nature of the cation involved in the quadruplex formation (12,13); (v) the molecular crowding (14); (vi) the presence of modified bases able to modulate the *syn*/*anti* equilibrium of the glycosidic bond conformation (15–22). Taking into account the close relationship between the strands orientation in a quadruplex structure and the glycosidic angles of the guanine residues, the regulation of this structural feature is one of the most used approaches to affect the folding topology of a quadruplex complex. For example, it is well known that 8-substituted purines facilitate the *syn* conformation (15–21) while RNA (22) and LNA (23) residues promote the *anti* conformation. In this context, with the aim to favour and stabilize a particular structure, several investigations on quadruplexes have been performed by introducing 8-bromo-2′-deoxyguanosine residues in sequence positions in which a guanine adopting a *syn* glycosidic conformation has been found or hypothesized (15–18). However, in NMR experiments, the use of this modified nucleotide in structural investigation shows a not negligible drawback due to the absence of any non-exchangeable protons at position 8, that does not allow the direct assessment of the glycosidic conformation, thus complicating the structure elucidation. In this context, the use of 8-methyl-2′-deoxyguanosine residues appears more appealing by virtue of the protons of methyl group that, thanks to the size similar to the bromine atom, is similarly able to promote a *syn* glycosidic conformation (19,20,24). Notwithstanding the advantageous properties of this base analogue, it is rarely used in the structural investigations of quadruplex complexes.

In this article, we report a structural study, based on NMR and CD spectroscopies, and molecular mechanics of all possible d(TG_3T) and d(TG_4T) analogues (Table 1), containing two 8-methyl-2′-deoxyguanosine residues. Particularly, the potential ability of these modified residues to orientate the strands and, then, to affect the folding topology of tetramolecular quadruplex structures has been investigated.

Table 1. Sequences of the ODNs studied and apparent melting temperatures ($T_{1/2}$) of the quadruplex structures formed by them

Name	Sequence (5′–3′)	$T_{1/2}$ (°C) at λ_{max} (CD)
TG_3T	TGGGT	45[a]
T12	TMMGT	57[a]
T13	TMGMT	34[a]
T23	TGMMT	ND
TG_4T	TGGGGT	65[b]
F12	TMMGGT	73[b]
F13	TMGMGT	47[b]
F14	TMGGMT	51[b]
F23	TGMMGT	52[b]
F24	TGMGMT	34[b]
F34	TGGMMT	24[b]

[a]70 mM K^+.
[b]70 mM Na^+.
M, 8-methyl-2′-deoxyguanosine; ND, not determined.

MATERIALS AND METHODS

Oligonucleotides synthesis and purification

The modified oligonucleotides reported in Table 1 were synthesized on a Millipore Cyclone Plus DNA synthesizer using solid phase β-cyanoethyl phosphoramidite chemistry at 15 μmol scale. The synthesis of the suitably protected 8-methyl-2′-deoxyguanosine-3′-phosphoramidite was performed following the synthetic strategy proposed by Khoda *et al*. (25). The oligomers were detached from the support and deprotected by treatment with concentrated aqueous ammonia at 55°C overnight.

The combined filtrates and washings were concentrated under reduced pressure, re-dissolved in H_2O, analysed and purified by high-performance liquid chromatography on a Nucleogel SAX column (Macherey–Nagel, 1000-8/46), using buffer A: 20 mM KH_2PO_4/K_2HPO_4 aqueous solution (pH 7.0) containing 20% (v/v) CH_3CN and buffer B: 1 M KCl, 20 mM KH_2PO_4/K_2HPO_4 aqueous solution (pH 7.0) containing 20% (v/v) CH_3CN; a linear gradient from 0 to 100% B for 30 min and flow rate 1 ml/min were used. The fractions of the oligomers were collected and successively desalted by Sep-pak cartridges (C-18). The isolated oligomers proved to be >98% pure by NMR.

NMR

NMR samples were prepared at a concentration of ~3 mM, in 0.6 ml (H_2O/D_2O 9:1 v/v) buffer solution having 10 mM KH_2PO_4/K_2HPO_4, 70 mM KCl and 0.2 mM EDTA (pH 7.0). All the samples were heated for 5–10 min at 80°C and slowly cooled (10–12 h) to room temperature. The solutions were equilibrated for several weeks at 4°C. The annealing process was assumed to be complete when ^{1}H-NMR spectra were superimposable on changing time. NMR spectra were recorded with Varian Unity INOVA 700 MHz and Varian Unity INOVA 500 MHz spectrometers. 1D proton spectra of the sample in H_2O were recorded using pulsed-field gradient DPFGSE (26) for H_2O suppression. ^{1}H-chemical shifts were referenced relative to external sodium 2,2-dimethyl-2-silapentane-5-sulfonate (DSS). Pulsed-field gradient DPFGSE sequence was used for NOESY (27) (180 and 80 ms mixing times) and TOCSY (28) (120 ms mixing time) experiments in H_2O. All experiments were recorded using STATES-TPPI (29) procedure for quadrature detection. In all 2D experiments, the time domain data consisted of 2048 complex points in t2 and 400–512 fids in t1 dimension. A relaxation delay of 1.2 s was used for all experiments.

CD spectroscopy

CD samples of modified oligonucleotides and their natural counterparts $[d(TGGGT)]_4$ and $[d(TGGGGT)]_4$ were prepared at a concentration of 1×10^{-4} M by using the buffer solution: 10 mM KH_2PO_4/K_2HPO_4, 70 mM KCl (or 10 mM NaH_2PO_4/Na_2HPO_4, 70 mM NaCl) and 0.2 mM EDTA (pH 7.0). In order to avoid discrepancies between NMR and CD results, we prepared CD samples by directly withdrawing the appropriate amounts from the

NMR tubes and diluting them just before the CD profile registration. CD spectra of all quadruplexes and CD melting curves were registered on a Jasco 715 CD spectrophotometer. For the CD spectra, the wavelength was varied from 220 to 320 nm at 100 nm/min scan rate, and the spectra recorded with a response of 16 s, at 2.0 nm bandwidth and normalized by subtraction of the background scan with buffer. The temperature was kept constant at 20°C with a thermoelectrically controlled cell holder (Jasco PTC-348). CD melting curves were recorded as a function of temperature from 20°C to 90°C for all quadruplexes at their maximum Cotton effect wavelengths. The CD data were recorded in a 0.1 cm path length cuvette with a scan rate of 10°C/h.

Gel electrophoresis

Modified oligonucleotides were analysed by non-denaturing PAGE. Samples in the NMR buffer (10 mM KH_2PO_4, 70 mM KCl and 0.2 mM EDTA, pH 7) were loaded on a 20% polyacrylamide gel containing Tris–Borate–EDTA (TBE) 2.5× and KCl 50 mM. The run buffer was TBE 1× containing 100 mM KCl. Single-strand samples were obtained by LiOH denaturation. For all samples, a solution of glycerol/TBE 1×100 mM KCl 2:1 was added just before loading. Electrophoresis was performed at 9.2 V/cm at a temperature close to 5°C. Bands were visualized by UV shadowing.

Molecular modelling

The main conformational features of quadruplexes **F12**, **F14**, **F24**, **F13**, **T12** and **T13** were explored by means of a molecular modelling study. The AMBER force field using AMBER 99 parameter set was used (30). In all cases, with the exception of **F13**, the initial coordinates for the starting models of the quadruplexes $[d(TGGGGT)]_4$ and $[d(TGGGT)]_4$ (for the G4-run and G3-run series, respectively) were taken from the NMR solution structure of the quadruplex $[d(TTGGGGT)]_4$ (Protein Data Bank entry number 139D), with one of the four available structures chosen randomly.

The initial $[d(TGGGGT)]_4$ G-quadruplex model was built by deleting the first thymidine residue in each of the four d(TTGGGGT) strands. The $[d(TGGGT)]_4$ model instead was obtained from the $[d(TGGGGT)]_4$ one by removing the 3′-end thymidine residue and replacing the final 3′-end 2′-deoxyguanosine with a thymidine residue. The complete structures of quadruplexes containing two 8-methyl-2′-deoxyguanosine residues were then built using the Biopolymer building tool of Discover by deleting two canonical 2′-deoxyguanosines at time for each strand and replacing them with 8-methyl-2′-deoxyguanosines for each model. According to NMR results, the 8-methyl-2′-deoxyguanosines were arranged in the *syn* conformation for M2 and in *anti* for M3 of **T12** and **F12** models. In the cases of **T13**, **F14** and **F24** both the modified residues were disposed in *syn*, according to NMR data. As far as **F13** is concerned, the initial coordinates for the starting model were taken from the NMR solution structure of the quadruplex $[d(GGGGTTTTGGGG)]_2$ (Protein Data Bank entry number 156D). By deleting the two central thymidine residues in the loop for both the d(GGGGTTTTG GGG) strands and by adding thymidine residues to the ends showing bare 2′-deoxyguanosine residues, a $[d(TGG GGT)]_4$ anti-parallel quadruplex structure was obtained. The complete structure containing two 8-methyl-2′-deoxyguanosine residues was then built using the Biopolymer building tool of Discover by deleting two canonical 2′-deoxyguanosines at time for each strand and replacing them with 8-methyl-2′-deoxyguanosines. In accordance to NMR data, the 8-methyl-2′-deoxyguanosines were arranged in the *syn* conformation for M2, M4, M8 and M10 residues of the **F13** model. The calculations were performed using a distance-dependent macroscopic dielectric constant of 4r, and an infinite cut-off for non-bonded interactions to partially compensate for the lack of solvent used (31). Using the steepest descent followed by quasi-NewtoneRaphson method (VA09A), the conformational energy of each complex was minimized until convergence to an RMS gradient of 0.1 kcal/mol Å was reached. Illustrations of structures were generated using the INSIGHT II program, version 2005 (Accelrys, San Diego, CA, USA). All the calculations were performed on a PC running Linux ES 2.6.9.

RESULTS

NMR experiments

In NMR investigations of G-quadruplex structures, the appearance of imino proton resonances in the region between 10.5 and 12.0 ppm in ^{1}H-NMR spectra can be considered as one of the distinctive features of complexes containing G-tetrads (32). Thus, the inspection of this region is commonly used both to assess whether the oligonucleotide adopts a unique or major structure and to provide insight into its symmetry.

The quite simple appearance of 1D spectra of ODNs **T12**, **T13**, **F12**, **F14** and **F24** (Figure 1) in K^+-containing solution (or in Na^+-containing solution) indicate that, under the conditions utilized, these oligomers form a main, well-defined hydrogen-bonded conformation consistent with highly symmetric G-quadruplex structures containing three (**T12** and **T13**) or four (**F12**, **F14** and **F24**) G-tetrads, thus showing all strands equivalent to each other. The ^{1}H-NMR spectrum of **T12** (500 MHz, $T = 25$°C) shows the presence of three main well-defined signals in the region 10.8–12.0 ppm, attributable to imino protons involved in Hoogsteen hydrogen bonds of G-quartets, and the presence of three singlets in the aromatic region belonging to the H8 unmodified guanine and to the two H6 thymine protons. Furthermore, four methyl resonances at ~1.6 ppm for the two T-CH_3 and at 2.2–2.5 ppm for the two M-CH_3 were observed (data not shown). In contrast, the 1D spectrum of **T13** at the same temperature shows the presence of two sets of signals in the aromatic range between 7.2 and 8.2 ppm, each formed by three signals slightly differing in intensity and

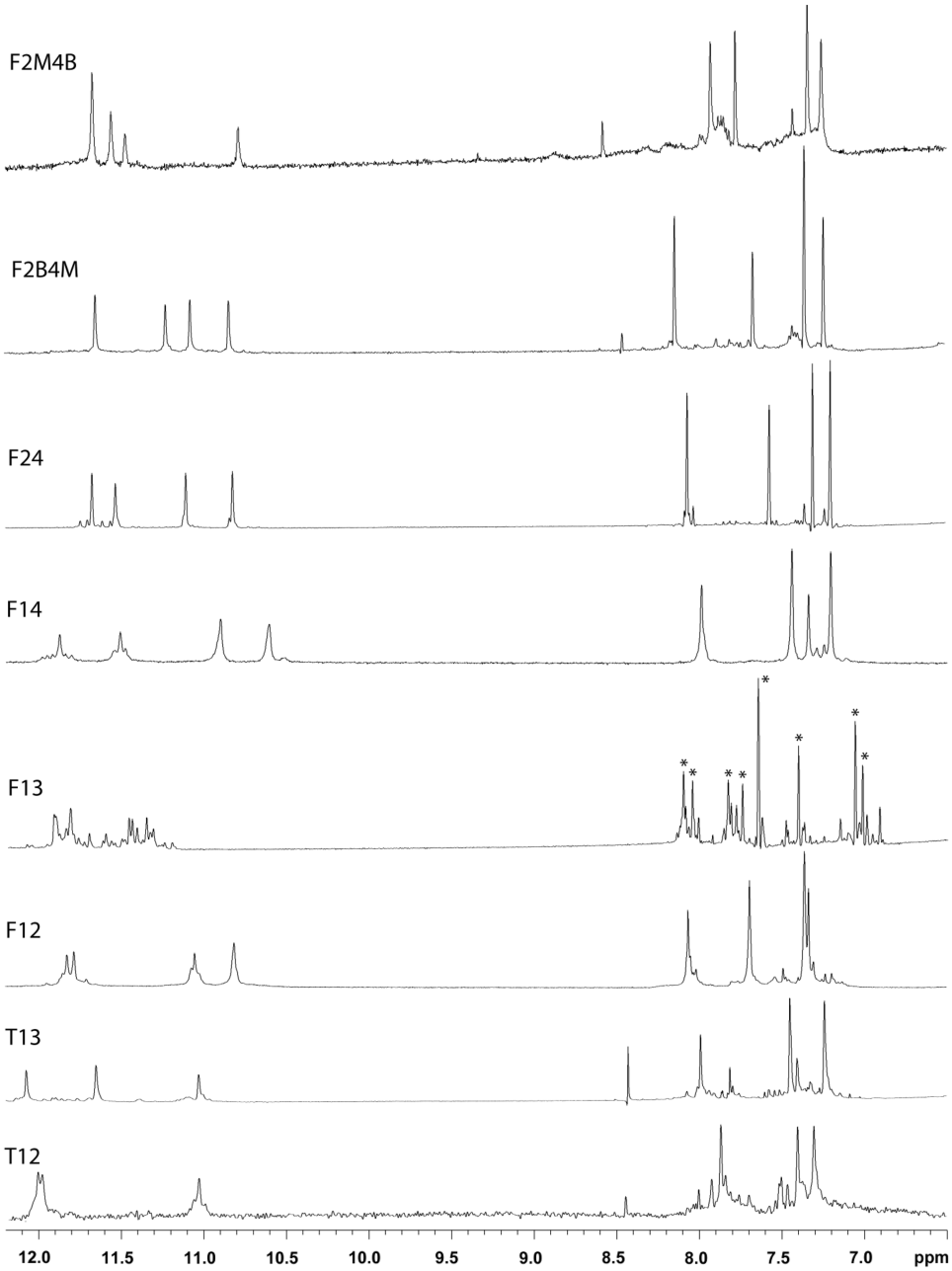

Figure 1. Aromatic and imino protons regions of the ^{1}H-NMR spectra (500 and 700 MHz) of **T12, T13, F12, F13, F14, F24, F2B4M** and **F2M4B** (Table 1) in 10 mM KH_2PO_4/K_2HPO_4, 70 mM KCl and 0.2 mM EDTA (pH 7.0). The temperature is 25°C for all samples except **T13** for which $T = 7$°C. For **F13** aromatic signals belonging to the major quadruplex structure are indicated by asterisks.

only three low imino peaks in the region 10.8–12.0 ppm (data not shown). By raising the temperature up to 50°C, three out of six signals gradually increased in intensity whereas the other three, along with the three imino peaks, progressively disappeared. Thus, at 50°C only three signals were present in the aromatic region of the ^{1}H-NMR spectrum, while no imino peaks were present. These data clearly indicate that at 50°C, **T13** is exclusively present as single strand that, at 25°C, coexists with nearly equally amounts of quadruplex structure. In view of detailed structural investigations, the quadruplex/single-strand ratio could be improved by decreasing the temperature to 7°C. In these conditions, the 1D spectrum shows that quadruplex **T13** possesses a 4-fold symmetry (as for **T12**), as indicated by the number of imino and aromatic protons (Figure 1).

Similarly, since ODNs **F12**, **F14** and **F24** contain four G-residues in their sequences, the quadruplex structures formed by them are characterized by all strands equivalent to each other. In fact, these ODNs show the presence of four imino proton resonances in the region between 10.5 and 12.0 ppm and four main singlets in the aromatic region between 7.0 and 8.0 ppm, two belonging to the two unmodified guanine H8 and two to the thymine H6

protons. The strands equivalence for quadruplexes formed by ODNs **F12**, **F14** and **F24** is further confirmed by the four methyl resonances in the range between 1.3 and 1.6 ppm attributable to the two T-CH_3 and between 2.2 and 2.5 ppm attributable to the two M-CH_3, that were observed for all three samples.

In contrast, the ^{1}H-NMR spectrum of **F13** (Figure 1) comes out more complicated than the previous ones. Indeed, in this case, the imino protons region is quite crowded and the number of signals suggests the presence in solution of several types of quadruplex structures. However, although the imino region does not allow a reliable estimation of the symmetry of the main structure, the number and the intensity of the aromatic protons signals would seem compatible with the presence of a major 2-fold symmetric structure, since eight main signals can be distinguished out of the other aromatic signals, belonging to minor quadruplex structures (Figure 1).

For the ODNs previously discussed, the exchange rates of the imino protons with solvent were qualitatively estimated by partially drying them in water and reconstituting them in D_2O. Periodic examination of the imino proton signals shows that they slowly exchange into D_2O solution compared to the NMR timescale, consistently with the high kinetic stability and low solvent accessibility of quadruplex structures (data not shown). As far as **T23**, **F23** and **F34** are concerned, the crowded imino and aromatic protons regions (Supplementary Figure S1) indicate the presence of several quadruplex structures, thus preventing us from further studying these samples in depth.

Since **T12**, **T13**, **F12**, **F14** and **F24** show 1D spectra clearly indicating that, under the conditions utilized, each ODN forms a main quadruplex structure, they have been further investigated by 2D NMR techniques. Their NOESY (Figures 2–4, Supplementary Figures S2 and S3) and TOCSY spectra have shown well-dispersed crosspeaks and consequently, both exchangeable and non-exchangeable protons could be nearly completely assigned following the standard procedures (Supplementary Tables S1–S3). As reported for other parallel quadruplex structures, the observed NOEs among G-H8 and T-H6 and their own H1′, H2′ and H2″ ribose protons and the H1′, H2′ and H2″ protons on the 5′-side suggest that all these quadruplexes assume a right-handed helical winding. As for the glycosidic torsion angles, for all the quadruplex structures formed by the five ODNs investigated, the presence of very weak NOEs between G-H8 and the corresponding ribose

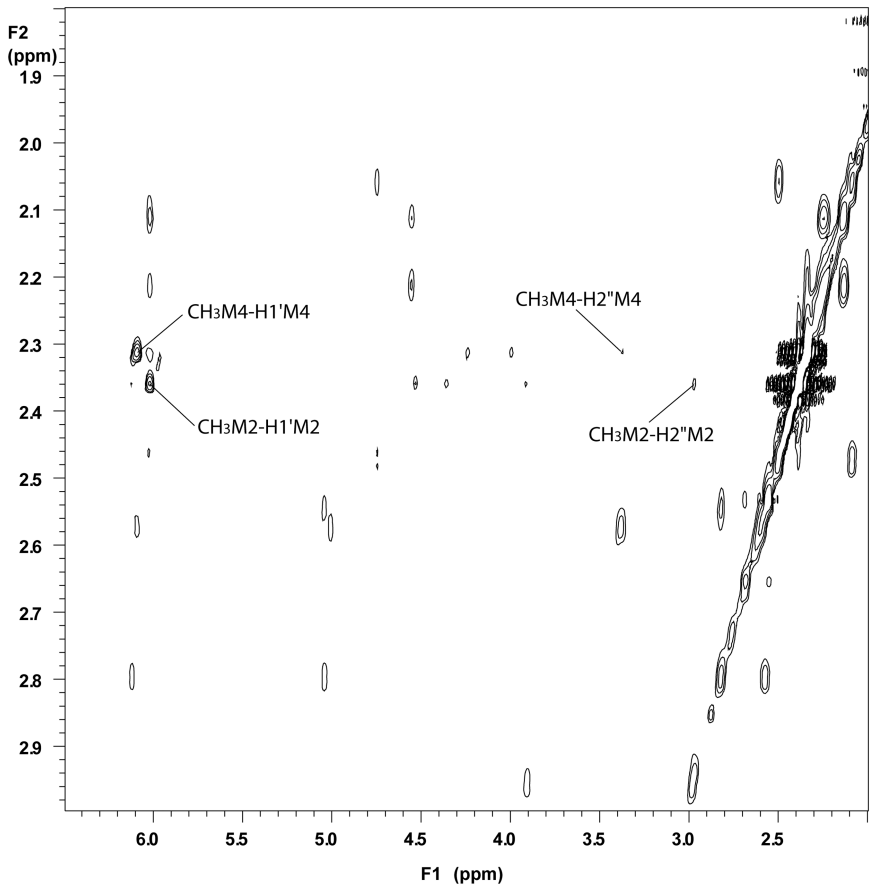

Figure 2. Expanded 2D NOESY spectrum of **T13** (700 MHz; 7°C; strand concentration ~3 mM; 10 mM KH_2PO_4/K_2HPO_4, 70 mM KCl and 0.2 mM EDTA, pH 7.0 in H_2O/D_2O 9:1; total volume 0.6 ml; mixing time 180 ms) correlating bases M CH_3-8 protons and sugar protons H1′ and H2″.

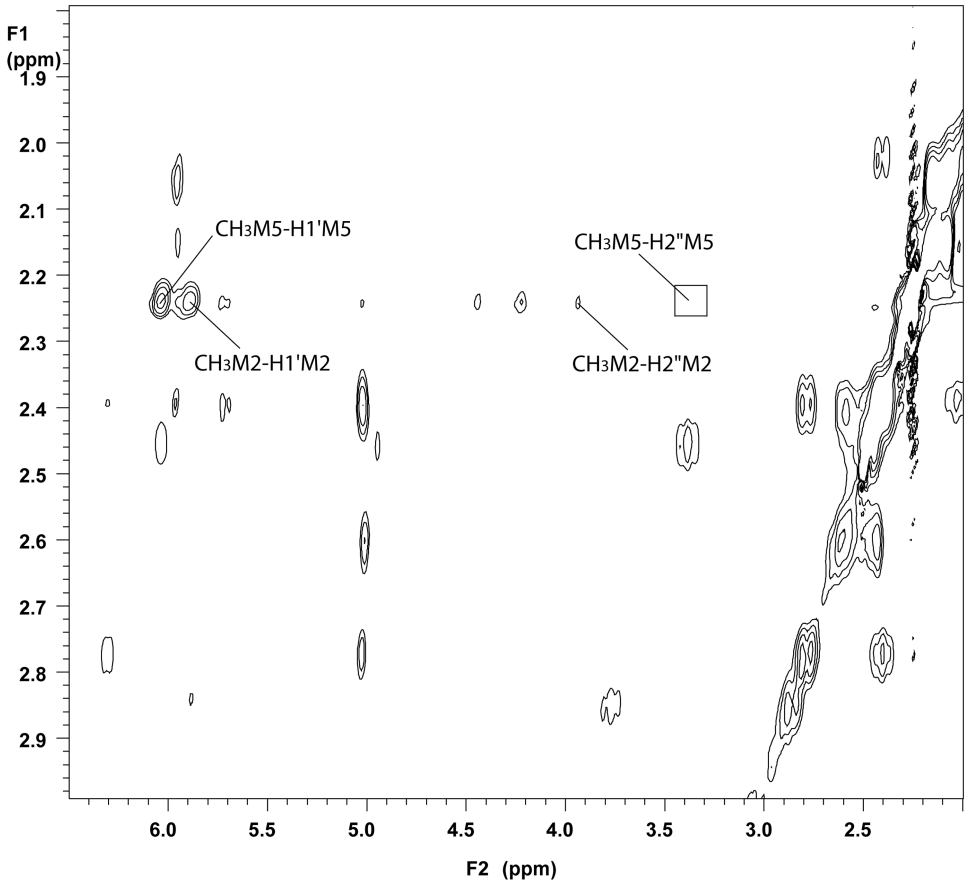

Figure 3. Expanded 2D NOESY spectrum of **F14** (500 MHz; 25°C; strand concentration ~3 mM; 10 mM KH_2PO_4/K_2HPO_4, 70 mM KCl and 0.2 mM EDTA, pH 7.0 in H_2O/D_2O 9:1; total volume 0.6 ml; mixing time 180 ms) correlating bases M CH_3-8 protons and sugar protons H1′ and H2″.

H1′ and of strong NOEs between G-H8 and ribose H2′ indicates that all unmodified guanosines possess *anti* glycosidic conformations, irrespectively of the ODN sequence. On the other hand, the behaviour of the M residues depends from the sequence context and for each structure it will be discussed separately.

In the quadruplex structure formed by **T12**, the first M residue in sequence shows a *syn* glycosidic conformation, as judged by the intense NOEs between the methyl group in 8-position and the H1′ sugar proton and the weaker crosspeak between methyl and H2″ (Supplementary Figure S2). In contrast, the second M residue adopts an *anti* glycosidic conformation as the unmodified guanosine (Supplementary Figure S2). A similar behaviour could be evidenced for the quadruplex structure formed by **F12**, in which only the 5′-end side modified guanosine shows a *syn* glycosidic conformation, while the other purines adopt *anti* glycosidic conformations (Supplementary Figure S3). NMR data for **T12** and **F12** are compatible with the formation of tetramolecular parallel quadruplex structures characterized by an all-*syn* tetrad at the 5′ end and two (for **T12**) or three (for **F12**) all-*anti* tetrads for the other purines (Figure 5). These results are in agreement with those obtained for monosubstituted TG_3T and TG_4T in the first and second positions, folding in quadruplex structures in which the modified guanosines form all-*syn* tetrads only if positioned at the 5′-end side (33,34).

NOESY examination about the quadruplex formed by ODN **T13** revealed that both the modified guanosines adopt *syn* glycosidic conformations (Figure 2), although this structure comes out less stable than quadruplex **T12** and their natural counterpart $[d(TGGGT)]_4$ (Table 1). In this case, NMR data are compatible with a tetramolecular parallel quadruplex in which two all-*syn* tetrads are present at the 3′- and 5′-end sides, while the central tetrad is formed by guanosines adopting *anti* glycosidic conformations (Figure 5).

Also in the case of ODN **F14**, NMR data (Figure 3) showed that both the modified residues adopt *syn* glycosidic conformations suggesting the formation of a tetramolecular parallel quadruplex characterized by two all-*syn* tetrads at the 5′- and 3′-end of the G tract (Figure 5). This arrangement is consistent with that of the quadruplex structures adopted by the monosubstituted ODNs TMGGGT and TGGGMT, in which the M residues form an all-*syn* tetrad in both cases (33).

Unfortunately, although also ODN **F24** forms a major quadruplex structure (Figure 1), as the previous ones, the chemical shift values of the methyl groups in 8-position

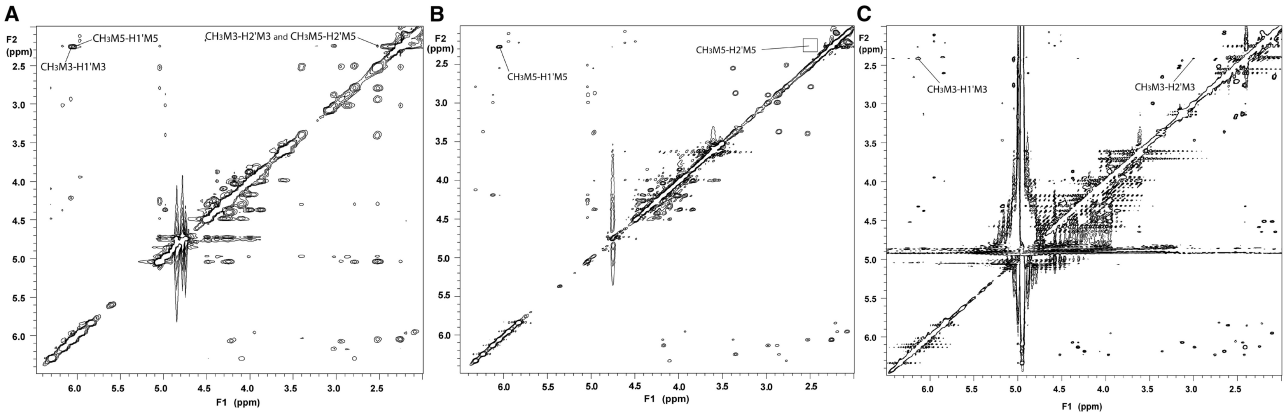

Figure 4. Expanded 2D NOESY spectra of **F24** (**A**), **F2B4M** (**B**) and **F2M4B** (**C**) (700 MHz; 25°C; strand concentration ~ 3 mM; 10 mM KH_2PO_4/K_2HPO_4, 70 mM KCl and 0.2 mM EDTA, pH 7.0 in H_2O/D_2O 9:1; total volume 0.6 ml; mixing time 180 ms) correlating bases M CH_3-8 protons and sugar protons H1′ and H2′.

and of the H1′ ribose protons are very similar for both the M residues (Figure 4A), resulting in strong NOE crosspeaks overlapped, that was not possible to resolve notwithstanding we tried to use higher magnetic field (700 MHz), different temperatures of acquisition and a more concentrated KCl solution (up to 140 mM) (data not shown).

Nevertheless, NOESY data indicate the presence of at least one *syn* M residue, although we are led to believe that both the modified guanosines adopt *syn* glycosidic conformations for the following reasons: (i) the presence of a large NOE crosspeak involving methyl groups and H1′ ribose protons of both M residues compared to a small NOE crosspeak involving methyl groups and H2′ ribose protons of the same residue, thus suggesting that both M residues adopt *syn* glycosidic conformations (Figure 4A); (ii) no sequential base-H1′, H2′, H2″ connectivities for both the 5′-GM-3′ steps could be observed, as already reported in other quadruplex structures containing 5′-G(*anti*)G(*syn*)-3′ steps (35). However, in order to support this assumption we have investigated the behaviour of two **F24** analogues expressly prepared, namely TGMGBT (**F2M4B**) and TGBGMT (**F2B4M**), in which M = 8-methyl-2′-deoxyguanosine and B = 8-bromo-2′-deoxyguanosine. Taking into account that the van der Waals radii of bromine atom and methyl group are comparable and, then, they are similarly able to promote the *syn* glycosidic conformation (24,36), quadruplex structures adopted by them are confidently very similar to that formed by **F24**. However, in the cases of **F2M4B** and **F2B4M**, the presence of only one 8-methyl-2′-deoxyguanosine for each sequence allowed us to observe individually the behaviour of the modified residues in the two quadruplex structures, thus circumventing the overlapping of the chemical shift values for methyl groups in 8-position and H1′ ribose protons observed in the case of **F24**. Both **F24** analogues are able to form a major quadruplex structure in solution (Figure 1). For both quadruplex structures formed by **F2M4B** and **F2B4M**, the presence of a strong NOEs between the methyl group in 8-position and the H1′ sugar proton compared to the weaker or absent crosspeaks between methyl and H2′ (Figure 4B and C), clearly point to M residues adopting *syn* glycosidic conformations. Since no interstrand NOEs have been observed for quadruplexes formed by **F24**, **F2M4B** and **F2B4M** the whole of the data clearly indicate that **F24** forms a tetramolecular parallel quadruplex, in which M residues and canonical guanosines adopt *syn* and *anti* glycosidic conformations, respectively, and the four strands are equivalent to each other, thus resulting in an unprecedented arrangement characterized by alternating all-*anti* and all-*syn* tetrads (Figure 5).

Although the ^{1}H-NMR spectrum of **F13** (Figure 1) appears quite complicated, thus suggesting the presence of several types of quadruplex structures, nevertheless the number of imino resonances could be compatible with a prevalent quadruplex structure characterized by a 2-fold symmetry. Even if NOESY (Figure 6) and TOCSY spectra only allowed us to partially assign the resonances (Supplementary Table S3), three important facts emerged from data: (i) the presence of four types of M residues (Figure 6A) all adopting *syn* glycosidic conformations and four types of canonical guanines all adopting *anti* glycosidic conformations; (ii) the presence of four types of thymines (Figure 6B); (iii) a NOESY crosspeak between T1-H6 and T6-CH_3 belonging to the same type of strand (Figure 6B). The first two data point to a complex containing two types of strands (A and B in Figure 5), thus supporting the presence of a major quadruplex structure with a 2-fold symmetry, while the latter datum would be compatible only with an anti-parallel strand arrangement. According to NMR and CD data (see below), we propose that **F13** forms a major tetramolecular anti-parallel quadruplex structure in which two adjacent strands run in one direction and the other strands run in the opposite one (A_2B_2 type) (37) (Figure 5). In fact, the whole of data allow us to rule out the parallel arrangement (A_4 type) (37) and the anti-parallel strand arrangements in which strands

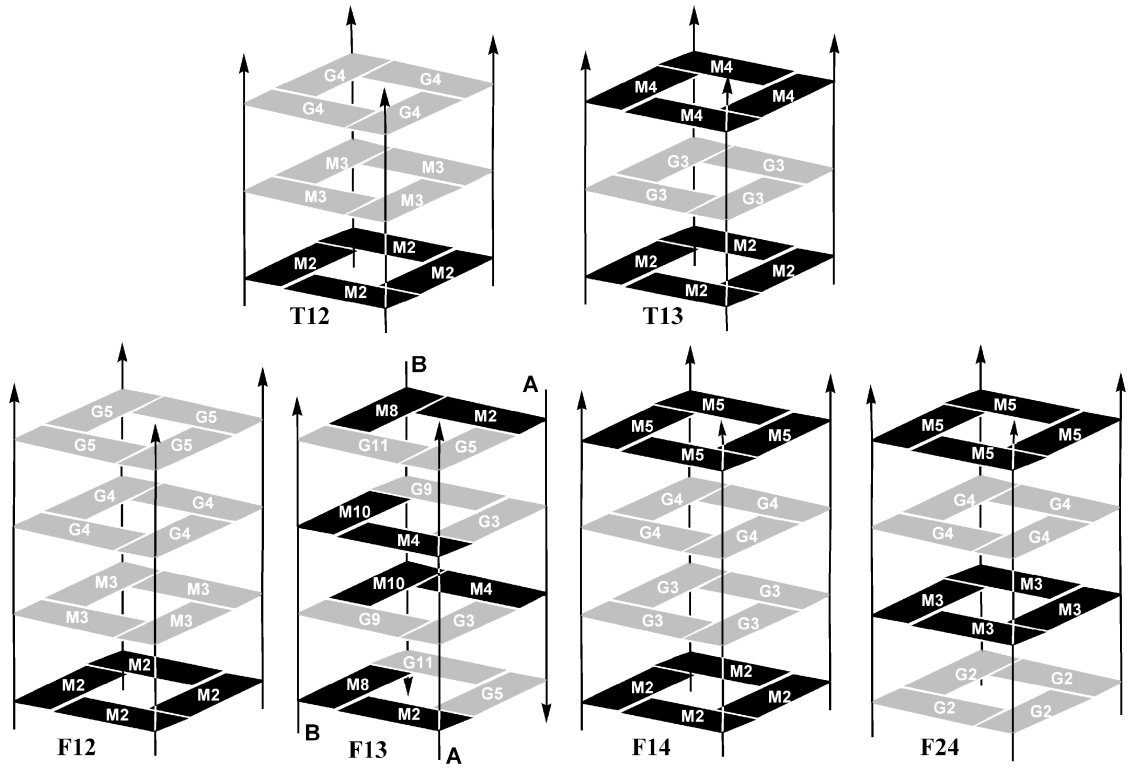

Figure 5. Schematic representation of the quadruplexes formed by **T12, T13, F12, F13, F14** and **F24**. *Anti* and *syn* residues are in grey and black, respectively. For each structure, equivalent residues are identically named. T residues have been omitted for clarity.

pointing in opposite directions alternate $(AB)_2$ type (37), for both of which an equivalence of the four strands would be expected (Supplementary Figure S4), and the mixed parallel–anti-parallel arrangement (A_3B type) (37) characterized by no symmetry.

CD spectroscopy and melting

This technique is often used to acquire preliminary data about the quadruplex folding topology or to confirm structural information obtained by other techniques. In this section, mainly we will discuss CD experiments of the ODNs that have proven by NMR to adopt a major quadruplex structure. The interpretation of the CD profiles could be facilitated taking into account a recent review in which a non-empirical chromophoric interpretation of CD spectra of quadruplex structures has been proposed (38). According to the authors, CD profiles can be interpreted in terms of different stacking orientation between adjacent G-tetrad irrespectively of the relative strands arrangement (parallel–anti-parallel). In fact, considering the heterotopic nature of the two faces of a G-tetrad, when two G-tetrads are stacked, each of them can interact with the adjacent one through the same (head-to-head, HH or tail-to-tail, TT) or the opposite (head-to-tail, HT) face resulting in a heteropolar or homopolar stacking, respectively (38).

In Figure 7A, CD spectra of quadruplexes **T12** and **T13** are shown compared with their natural counterpart. The CD profile of **T12** exhibits two positive bands at 246 and 295 nm and two negative ones at 230 and 266 nm. According to the NMR results the proposed structure is characterized by one heteropolar (HH) and one homopolar (HT) stacking (Figure 5), as for quadruplex structures formed by ODNs TBGGT (tetramolecular, B = 8-bromo-2′-deoxyguanine) (39), TMGGT (tetramolecular) (33) and $G_3T_4G_3$ (bimolecular) (40–42) that show quite similar CD profiles (38).

On the other hand, CD spectrum of **T13** shows two positive bands at 244 and 297 nm and a large negative band at 265 nm. The quadruplex structure proposed for **T13** (Figure 5) shows two heteropolar (HH) stacks. In 'antiparallel' quadruplexes, as those formed by ODNs $G_4T_4G_4$ (bimolecular) (43,44) and $G_4T_2G_4TGTG_4T_2G_4$ (monomolecular) (44), G-tetrads are piled only through heteropolar stackings. In fact, their CD profiles are almost superimposable to that of **T13**, this datum corroborating the quadruplex structure proposed for this ODN according to the NMR experiments.

The main features of CD spectrum of **T23** (Supplementary Figure S5) are a positive band at 257 nm and a negative band at 291 nm that would suggest a dominance of 'parallel' structures containing homopolar stackings. However, in this case, as underlined before in the NMR section, the large amount of random coil and the absence of a major quadruplex structure make impracticable to obtain reliable structural information from the CD spectrum.

Figure 7B shows CD spectra of **F12** and **F14** compared with their natural counterpart. CD profile of quadruplex **F12** displays two positive bands at 261 and 299 nm and a

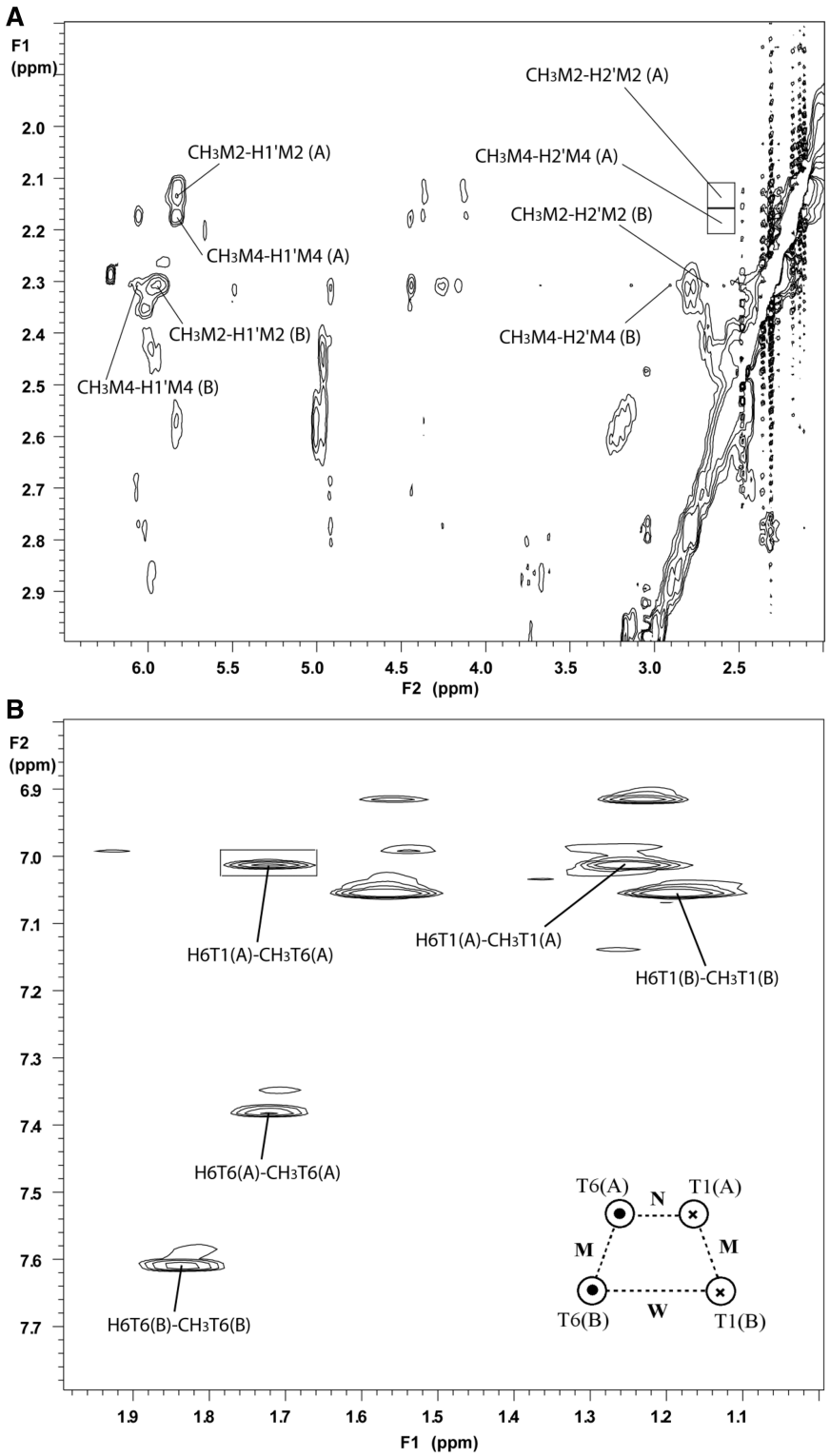

Figure 6. (A) Expanded 2D NOESY spectrum of **F13** (700 MHz; 25°C; strand concentration ~3 mM; 10 mM KH_2PO_4/K_2HPO_4, 70 mM KCl and 0.2 mM EDTA, pH 7.0 in H_2O/D_2O 9:1; total volume 0.6 ml; mixing time 180 ms) correlating bases M CH_3-8 protons and sugar protons H1′ and H2′. **(B)** Expanded 2D NOESY spectrum of **F13** correlating thymines (T) CH_3-5 and H6. The box indicates NOE contact between H6T1 (strand A) and CH_3T6 (strand A). The inset shows a schematic representation of the upside view of the suggested quadruplex structure for **F13.** The two types of strands are labelled A and B. Dots and crosses indicate 3′- and 5′-ends, respectively. N, M and W indicate narrow, medium and wide grooves, respectively.

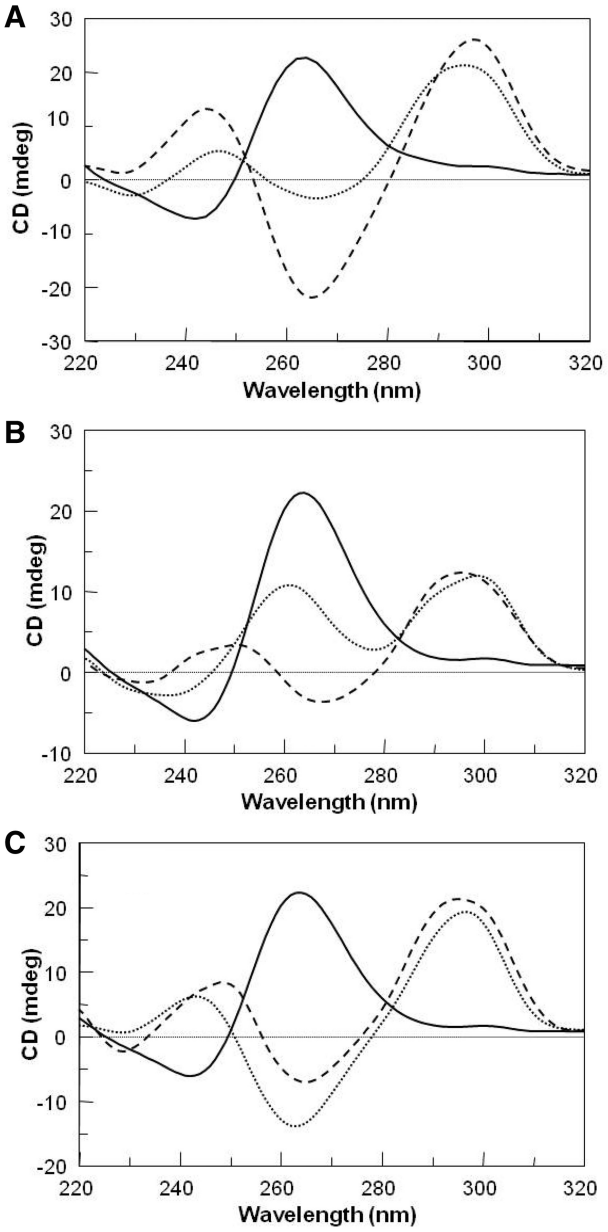

Figure 7. CD spectra of ODNs (**A**) $\mathbf{TG_3T}$ (solid lines), **T12** (dotted lines) and **T13** (dashed lines); (B) $\mathbf{TG_4T}$ (solid lines), **F12** (dotted lines) and **F14** (dashed lines); (C) $\mathbf{TG_4T}$ (solid lines), **F13** (dotted lines) and **F24** (dashed lines) at 20°C, strand concentration 0.1 mM, 10 mM KH_2PO_4/K_2HPO_4, 70 mM KCl and 0.2 mM EDTA, pH 7.0.

negative band at 237 nm. NMR experiments pointed to a tetramolecular parallel quadruplex structure in which the first tetrad is all-*syn* while the other ones are all-*anti*, thus leading to one heteropolar (HH) and two homopolar (HT) stackings (Figure 5). This tetrads arrangement occurs in quadruplex formed by ODN TMGGGT (34) that shows a CD spectrum almost superimposable to that of quadruplex **F12**, apart for the difference in intensity of the band at 297 nm that could be tentatively ascribed to the presence of two M residues in **F12**. On the other hand, the same number of heteropolar and homopolar stacks are present in quadruplexes proposed for some ODNs containing inversion of polarity sites as $^{3'}TGG^{5'}$-$^{5'}GGT^{3'}$ (two HT and one HH stacking) and $^{5'}TGG^{3'}$-$^{3'}GGT^{5'}$ (two HT and one TT stacking) that show CD profiles similar to that of **F12** (38,45).

CD spectrum of quadruplex **F14** shows mainly two positive bands at 250 and 296 nm, and two negative bands at 231 and 268 nm. In this case, NMR results have strongly suggested a quadruplex structure characterized by two heteropolar (one HH and one TT) and one homopolar stacks (Figure 5) that, unfortunately, results in an unprecedented tetrads arrangement, thus preventing us to directly compare CD profiles of **F14** and those of similar quadruplex structures. In spite of this, a comparison of CD spectra of **F14** and **T13** (forming a quadruplex with only heteropolar stackings) clearly shows that the negative band ~265 nm (distinctive of heteropolar stackings) (38) is relatively less pronounced for **F14**, as expected for a quadruplex structure in which two heteropolar and one homopolar stacks occur. Therefore, also the CD profiles of **F14** is in good agreement with the proposed quadruplex structure according to the NMR results.

The CD spectrum of ODN **F13** (Figure 7C) supports the assumption based on NMR data previously described, since it shows two positive bands at 243 and 297 nm and a strong negative band at 263 nm, which matches a CD profile typical of an 'anti-parallel' quadruplex structure characterized only by heteropolar stackings. More significantly, CD spectrum of **F13** is essentially superimposable to that of the bimolecular quadruplex $[d(G_4T_4G_4)]_2$ (44) that folds in an anti-parallel arrangement in which two adjacent strands run in one direction and the other ones run in the opposite direction (A_2B_2 type) (37), thus matching the anti-parallel quadruplex structure proposed for **F13** (Figure 5).

Also, in the case of **F24**, its CD spectrum corroborates the conclusions deriving from NMR experiments. In fact, its CD profile exhibits two positive bands at 248 and 295 nm and two negative bands at 228 and 265 nm suggesting the presence of only heteropolar stackings [compare CD profiles of **F24** with the heteropolar stacked quadruplexes **T13**, $[d(G_4T_4G_4)]_2$ (43,44) and $d(G_4T_4G_4TGTG_4T_4G_4)$ (44)].

The CD profiles for **F23** and **F34** (Supplementary Figure S5) appear very similar to that of **F14** (Figure 7B). However, in these cases, as for **T23** and in contrast to **F14**, NMR data do not support the presence of a major quadruplex structure, thus making impracticable the acquisition of reliable information from the CD spectra.

In order to estimate thermal stability of the quadruplex structures formed by the modified ODNs, melting and annealing CD measurements were performed in comparison with $[d(TGGGT)]_4$ and $[d(TGGGGT)]_4$ under the same experimental conditions. Since for most of the modified TGGGGT no melting curves have been observed in potassium solution, experiments were performed in potassium buffer for modified TGGGT and in sodium buffer for modified TGGGGT. In the latter case, the CD profiles in Na^+ solution (data not shown) were

very similar to those in K^+ solution, thus indicating no significant structural differences between quadruplexes formed in sodium and potassium solutions. As expected, due to the tetramolecular nature of the complexes, severe hysteresis phenomena were observed for all ODNs (data not shown), despite the very slow scan rates used (10°C/h), thus indicating that the systems were not at equilibrium. However, we obtained good melting profiles (data not shown) that allowed us to determine the apparent melting temperatures ($T_{1/2}$) usually considered quite useful to compare thermal stabilities (46). The apparent melting temperatures of the modified ODNs were listed in Table 1. The $T_{1/2}$ of quadruplexes formed by ODNs **T12** and **F12** come out higher than their natural counterparts, thus confirming results obtained for modified ODNs TGG GT and TGGGGT containing only one M residue (33,34) in which the introduction of an 8-methyl-2′-deoxyguanosine at the 5′-end of the G-run results in an improved thermal stability, while the same modification at the second position does not affect significantly the structural properties compared to the natural sequences. On the other hand, for parallel quadruplex structures (**T12**, **T13**, **F12**, **F14** and **F24**), data clearly show that thermal stability decreases as the position of the M residues approaches the 3′-end, this result is also in good agreement with data obtained for modified ODNs TGGGT and TGGGGT containing only one M residue (33,34). The $T_{1/2}$ of quadruplexes formed by ODNs **F23** and **F34** are in good agreement with this trend as well, although in these cases, NMR data have not allowed us to gain any insights into their structural properties.

Gel electrophoresis

In order to estimate the molecularity of the complexes, we performed PAGEs of the modified TGGGT and TGGGG T quadruplexes compared with their natural counterparts $[d(TGGGT)]_4$ and $[d(TGGGGT)]_4$, respectively (Supplementary Figure S6). For most of the cases, the migration of the non-denaturated samples appears undoubtedly slower than those of the corresponding single strands, clearly showing the presence of multimolecular complexes. However, samples of **T12**, **F12** and **F13** were able to completely renaturate in the PAGE conditions, while for **F14** and **F24** a partial renaturation occurs during the electrophoretic run. On the other hand, in the case of **T23**, we have been able to observe only the single strand probably due to the inadequate amount of quadruplex structure present in solution, as suggested by the ^{1}H-NMR spectrum (Supplementary Figure S1). For both the series, modified TGGGT and TGGGGT quadruplexes migrate faster than their natural counterparts. This effect has been already observed for the electrophoretic motilities of the monosubstituted series (34). In several cases, no structures larger than tetramolecular quadruplexes could be detected. However, in the cases of **T13**, **F24** and **F34,** PAGEs show minor amounts of slower migrating species probably attributable to higher order structures.

Molecular modelling

Literature data concerning similar structures and NMR data collected in this study allowed us to obtain molecular models for quadruplexes formed by **T12**, **T13**, **F12**, **F13**, **F14** and **F24** and compare their structures. Concerning the molecular models of **T12** and **F12** (Figure 8), it can be noted that all purine bases involved in the formation of G-tetrads, including the modified residues M, are able to form well-defined and planar tetrads and the resulting quadruplex structures show an optimal right-handed helical twist and a 4-fold symmetry. In both quadruplexes, the M residues of the first tetrad assume a perfectly *syn* glycosidic conformation without causing any distortions of the backbone and resulting in a good stacking with the underneath all-*anti* M-tetrad. As far as **F24** (Figure 8), **F14** and **T13** (Supplementary Figure S7) are concerned, as expected, also in these cases all structures show a right-handed helical backbone geometry, in which the strands are equivalent to each other without any severe distortions, notwithstanding the unusual presence of two all-*syn* M-tetrads. Nevertheless, it is interesting to note that in both **F14** and **F24** structures, the first two tetrads at the 5′-end have an almost planar conformation, while the remainder tetrads exhibits a bowl shape, more pronounced at 3′-end. In particular, this phenomenon is more marked in the case of **T13**, in which the M residues near to the 3′-end are only partially engaged in the tetrad and then, more accessible to the solvent, according to NMR data recorded at 25°C (data not shown). The general structural features of the molecular models discussed above are in good agreement with the data obtained from the apparent melting temperature measurements, clearly indicating that quadruplexes **T12** and **F12** are more stable than structures formed by their homologous ODNs (Table 1). In the case of **F13**, NMR and CD data suggest that the quadruplex structure exhibits adjacent strands parallel in pair, with alternating 5′-*syn–anti–syn–anti*-3′ residues along the G-tract, thus resulting in four *syn–syn–anti–anti* tetrads in which M residues and canonical guanosines adopt *syn* and *anti* glycosidic conformations, respectively. This arrangement implies a peculiar feature: the presence of two symmetric medium grooves, one narrow groove and one wide groove, with the width being determined by the relative orientations of the sugar moieties. In our model (Figure 8), four methyl groups of the M residues lie perfectly in the two medium grooves (two methyl groups for each groove), while the remaining four methyl groups lie in the wide groove. It is noteworthy that this structural arrangement does not imply any severe distortion of the tetramolecular complex, which strictly resembles that of the diagonally looped structure showed by the *Oxytricha* telomere repeat $[d(G_4T_4G_4)]_2$ in solution (47).

DISCUSSION

Since the first decade after the discovery of G-quadruplexes, these structures have been successfully investigated by introducing modified guanines in the

DNA sequence and observing the effects on the structural features and thermodynamic stability. In this context, the C8 position of the guanine is particularly suitable, mainly for two reasons: (i) it does not affect the Watson–Crick and Hoogsteen pairing distinctive of a G-tetrad; and (ii) a bulky substituent in this position shifts the equilibrium conformation around the glycosidic bond to favour the *syn* conformation. If, on one hand, the replacement of *syn* guanines by 8-substituted analogues has proven to be rather useful in stabilizing the structure, on the other hand, the same replacement concerning *anti* guanines decreases the stability, thus suggesting the use of a 8-substituted guanosine as a chemical probe (48). A noteworthy exception to this rule concerns the introduction of 8-substituted guanosine analogues in parallel quadruplex structures in which, in general, all G-residues adopt *anti* glycosidic conformation. Several authors report that the insertion of a residue of 8-bromo-2′-deoxyguanosine (49), 8-amino-2′-deoxyguanosine (50) or 8-methyl-2′-deoxyguanosine (34) at the 5′-end of the G-run in tetramolecular quadruplexes as $[d(TG_nT)]_4$ ($n = 3–5$) increases the thermal stability and accelerates the formation of the complexes. Interesting results regarding the structural features come out, as well. For example, in quadruplex structures $[d(TG_3T)]_4$ and $[d(TG_4T)]_4$ the effects of an 8-methyl-2′-deoxyguanosine incorporation are sequence dependent (34): the replacement of the first guanosine in sequence results in the formation of an all-*syn* tetrad never observed before in solution, while the replacement of the second guanosine in sequence, surprisingly, does not affect the original *anti* preference of the residue, notwithstanding the presence of the methyl group in the 8 position usually promoting a *syn* glycosidic conformation. Since, to the best of our knowledge, only one investigation concerning the introduction of more than one 8-substituted deoxyguanosine analogues in parallel quadruplexes has been reported to date (51), we have explored the ability to form G-quadruplexes and their structural properties of ODNs analogues of TG_3T and TG_4T in which two canonical guanines have been replaced by 8-methyl-2′-deoxyguanosine residues (Table 1). Results obtained for ODNs **T12** and **F12** confirm the findings obtained for ODNs analogues of TG_3T and TG_4T in which one canonical guanine has been replaced by an 8-methyl-2′-deoxyguanosine residue (33,34): these ODNs adopt a tetramolecular parallel G-quadruplex characterized by an all-*syn* M-tetrad stacked to an all-*anti* M-tetrad. In particular, it is noteworthy that **F12** forms this unusual structure, although it could potentially adopt several strand orientations in all of which the canonical guanines and the 8-methyl-2′-deoxyguanosine residues adopt *anti* and *syn* glycosidic conformations, respectively (Supplementary Figure S8). However, it should be noted that all these structures would be characterized by four *syn–syn* steps that, among the four possible base pair step patterns (namely, *syn–anti*, *anti–anti*, *anti–syn* and *syn–syn*), have suggested to be the less stable, according to a recent study on MD simulation and free energetic analyses for simplified two quartet $[d(GG)]_4$ models (52).

The case of **T13** is particularly remarkable. As a matter of fact, it adopts a parallel G-quadruplex structure containing two all-*syn* M-tetrads. At the best of our knowledge, this is the first G-quadruplex in which it has been ascertained that the *syn* purines exceed in number the *anti* purines, even if this structure comes out the less stable in the series.

F14 also prefers a parallel folding topology. However, in contrast to **F12**, it should be noted that no anti-parallel G-quadruplex structures would be compatible with strand orientation characterized by canonical guanines adopting *anti* conformations and M residues adopting *syn* conformations; although, in principle, M residues could adopt *anti* conformations, as for the second guanosine in the G-quadruplex formed by **F12**.

The cases of **F13** and **F24** are worth to be discussed together. In fact, both the ODNs show a sequence in which canonical G and modified M residues alternate. In principle, these ODNs would be able to form all types of tetramolecular non-parallel G-quadruplex structures characterized by canonical G and the M residues adopting *anti* and *syn* glycosidic conformations, respectively (Supplementary Figures S4 and S9). However, their behaviour appears quite different. As a matter of fact, **F24** forms an unprecedented parallel G-quadruplex structure characterized by alternating all-*anti* G-tetrads and all-*syn* M-tetrads, while NMR, CD and molecular modelling data strongly suggest that **F13** adopts a major structure with

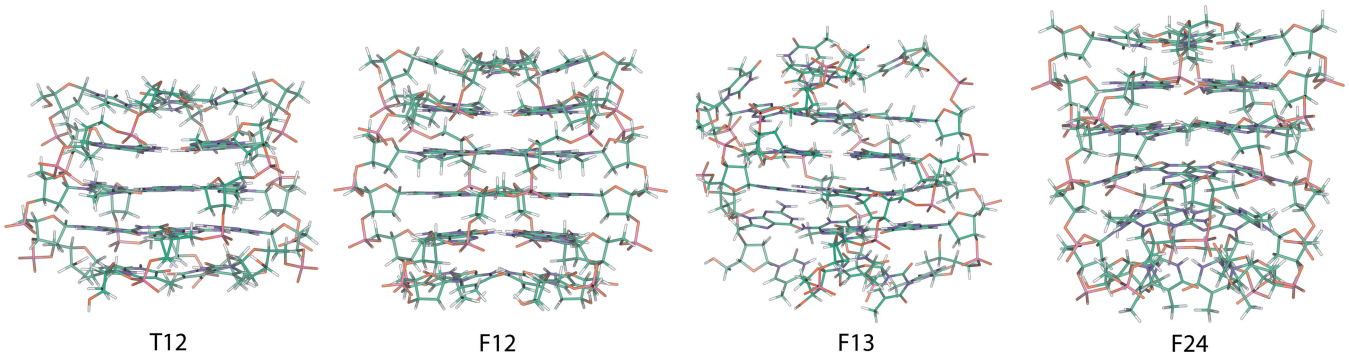

Figure 8. Molecular models of the quadruplexes formed by ODNs **T12, F12, F13** and **F24**. The structures are oriented with the 5′-end upward (carbons, green; nitrogens, blue; oxygens, red; hydrogens, white; phosphorus, pink).

strands being parallel in pairs (A_2B_2 type) (37) and characterized by four *syn–syn–anti–anti* tetrads in which canonical G adopt *anti* conformations and M residues adopt *syn* conformations. This strands arrangement is similar to that observed for bimolecular G-quadruplexes containing four G-tetrads, formed by the two-repeat *Tetrahymena* telomeric d(TG_4TTG_4T) (53) sequence and by the *Oxytricha* telomere repeat d($G_4T_4G_4$) (47) in solution. It should be noted that all the anti-parallel quadruplex structures containing two or four stacked tetrads [both A_2B_2 and $(AB)_2$ types] (37) described in literature to date, are characterized by 5′-ends of the quadruplex stem starting with a *syn* residue (12,47,53–56). Furthermore this feature is also present for most of the non-parallel quadruplex structures containing three tetrads (17,57–65). This characteristic has been successfully exploited in the design of a new G-quadruplex topology through glycosidic bond angles and by controlling the fold through the length of the loops (66). The quadruplex structure proposed for **F13** (Figure 5) is in good agreement with the literature data on other anti-parallel quadruplexes, since the G-run of **F13** starts with a M residue that favours a *syn* glycosidic conformation. To the best of our knowledge, this is the first tetramolecular anti-parallel quadruplex structure strongly suggested on the basis of NMR and CD data, even though some authors have proposed the formation of a A_2B_2 type anti-parallel tetrameric quadruplex for the double repeat of human telomere d(TTAGGGTTAGGG) in Na^+ solution (67). On the other hand, although the sequence of **F24** is also composed by alternating canonical guanines and modified M residues, it prefers to adopt a parallel strand arrangement. This datum could be explained taking into account that the G-run of **F24** does not start with a M residue prone to assume a *syn* conformation, as in the case of **F13**, thus making the formation of an anti-parallel quadruplex structure not particularly favourable.

The results described in this investigation supply further data to the structural features of the quadruplex complexes concerning the relative strands orientation and the glycosidic conformation of the bases and expands the known structural motifs of the DNA G-quadruplexes. In particular, the ability of two 8-methyl-2′-deoxyguanosine residues, introduced in different sequence positions, to orientate the strands in parallel quadruplex structures has been investigated: ODNs containing two modified bases are able to form both parallel and anti-parallel quadruplex structures. The possibility of introducing into the grooves of a quadruplex structure methyl groups that are potentially able to establish hydrophobic interactions may be of interest in the area of anti-HIV aptamers forming tetramolecular quadruplexes such as the phosphorothioate $[d(T_2G_4T_2)]_4$ (68) and $[d(GAGGGT)]_4$ analogues (2) in order to improve the affinity and specificity to their target. Furthermore, some quadruplexes examined in this research could be considered good models for the study of the interaction between groove binder compounds and quadruplex of biological interest (69).

SUPPLEMENTARY DATA

Supplementary Data are available at NAR Online: Supplementary Tables S1-S3, Supplementary Figures S1–S9.

ACKNOWLEDGEMENTS

The authors are grateful to ‘Centro di Servizi Interdipartimentale di Analisi Strumentale’, C.S.I.A.S., for supplying NMR facilities and for technical support in CD measurements. The authors are also grateful to Alessia Borrone, Maria Reale, Pasquale Paciello and Luisa Cuorvo for their collaboration.

FUNDING

Ministero dell’Istruzione, Università e Ricerca (MIUR). Funding for open access charge: Università degli Studi di Napoli Federico II Dipartimento di Chimica delle Sostanze Naturali.

Conflict of interest statement. None declared.

REFERENCES

1. Huppert,J.L. and Balasubramanian,S. (2005) Prevalence of quadruplexes in the human genome. *Nucleic Acids Res.*, **33**, 2908–2916.
2. Pedersen,E.B., Nielsen,J.T., Nielsen,C. and Filichev,V.V. (2011) Enhanced anti-HIV-1 activity of G-quadruplexes comprising locked nucleic acids and intercalating nucleic acids. *Nucleic Acids Res.*, **39**, 2470–2481.
3. Reyes-Reyes,E.M., Teng,Y. and Bates,P.J. (2010) A new paradigm for aptamer therapeutic AS1411 action: uptake by macropinocytosis and its stimulation by a nucleolin-dependent mechanism. *Cancer Res.*, **70**, 8617–8629.
4. Pasternak,A., Hernandez,F.J., Rasmussen,L.M., Vester,B. and Wengel,J. (2011) Improved thrombin binding aptamer by incorporation of a single unlocked nucleic acid monomer. *Nucleic Acids Res.*, **39**, 1155–1164.
5. Coppola,T., Varra,M., Oliviero,G., Galeone,A., D’Isa,G., Mayol,L., Morelli,E., Bucci,M.R., Vellecco,V., Cirino,G. *et al.* (2008) Synthesis, structural studies and biological properties of new TBA analogues containing an acyclic nucleotide. *Bioorg. Med. Chem.*, **16**, 8244–8253.
6. Poon,L.C.-H., Methot,S.P., Morabi-Pazooki,W., Pio,F., Bennet,A.J. and Sen,D. (2011) Guanine-rich RNAs and DNAs that bind heme robustly catalyze oxygen transfer reactions. *J. Am. Chem. Soc.*, **133**, 1877–1884.
7. Wu,Y. and Brosh,R.M. Jr (2010) G-quadruplex nucleic acids and human disease. *FEBS J.*, **277**, 3470–3488.
8. Neidle,S. and Balasubramanian,S. (2006) *Quadruplex nucleic acids*. RSC Publishing, London.
9. Risitano,A. and Fox,K.R. (2004) Influence of loop size on the stability of intramolecular DNA quadruplexes. *Nucleic Acids Res.*, **32**, 2598–2606.
10. Rachwal,P.A., Findlow,I.S., Werner,J.M., Brown,T. and Fox,K.R. (2007) Intramolecular DNA quadruplexes with different arrangements of short and long loops. *Nucleic Acids Res.*, **35**, 4214–4222.
11. Guedin,A., De Cian,A., Gros,J., Lacroix,L. and Mergny,J.-L. (2008) Sequence effects in single-base loops for quadruplexes. *Biochimie*, **90**, 686–696.
12. Hu,L., Lim,K.W., Bouaziz,S. and Phan,A.T. (2009) *Giardia* telomeric sequence $d(TAGGG)_4$ forms two intramolecular G-quadruplexes in K^+solution: effect of loop length and sequence on the folding topology. *J. Am. Chem. Soc.*, **131**, 16824–16831.

13. Wang,Y. and Patel,D.J. (1993) Solution structure of the human telomeric repeat d[$AG_3(T_2AG_3)_3$] G-tetraplex. *Structure*, **1**, 263–282.
14. Heddi,B. and Phan,A.T. (2011) Structure of human telomeric DNA in crowded solution. *J. Am. Chem. Soc.*, **133**, 9824–9833.
15. Abu-Ghazalah,R.M., Irizar,J., Helmy,A.S. and MacGregor,R.B. (2010) A study of the interactions that stabilize DNA frayed wires. *Biophy. Chem.*, **147**, 123–129.
16. Sannohe,Y., Sato,K., Matsugami,A., Shinohara,K., Mashimo,T., Katahira,M. and Sugiyama,H. (2009) The orientation of the ends of G-quadruplex structures investigated using end-extended oligonucleotides. *Bioorg. Med. Chem.*, **17**, 1870–1875.
17. Matsugami,A., Xu,Y., Noguchi,Y., Sugiyama,H. and Katahira,M. (2007) Structure of a human telomeric DNA sequence stabilized by 8-bromoguanosine substitutions, as determined by NMR in a K^+ solution. *FEBS J.*, **274**, 3545–3556.
18. Xu,Y., Noguchi,Y. and Sugiyama,H. (2006) The new models of the human telomere d[$AGGG(TTAGGG)_3$] in K^+ solution. *Bioorg. Med. Chem.*, **14**, 5584–5591.
19. He,G.-X., Krawczyk,S.H., Swaminathan,S., Shea,R.G., Dougherty,J.P., Terhorst,T., Law,V.S., Griffin,L.C., Coutre,S. and Bischofberger,N. (1998) N2- and C8-substituted oligodeoxynucleotides with enhanced thrombin inhibitory activity in vitro and in vivo. *J. Med. Chem.*, **41**, 2234–2242.
20. Xu,Y. and Sugiyama,H. (2006) Formation of the G- quadruplex and i-motif structures in retinoblastoma susceptibility genes (Rb). *Nucleic Acids Res.*, **34**, 949–954.
21. Virgilio,A., Esposito,V., Randazzo,A., Mayol,L. and Galeone,A. (2005) Effects of 8-methyl-2′-deoxyadenosine incorporation into quadruplex forming oligodeoxyribonucleotides. *Bioorg. Med. Chem.*, **13**, 1037–1044.
22. Tang,C.-F. and Shafer,R.H. (2006) Engineering the Quadruplex Fold: Nucleoside Conformation Determines Both Folding Topology and Molecularity in Guanine Quadruplexes. *J. Am. Chem. Soc.*, **128**, 5966–5973.
23. Pradhan,D., Hansen,L.H., Vester,B. and Petersen,M. (2011) Selection of G-Quadruplex Folding Topology with LNA-Modified Human Telomeric Sequences in K^+ Solution. *Chem. Eur. J.*, **17**, 2405–2413.
24. Xu,Y., Ikeda,R. and Sugiyama,H. (2003) 8-Methylguanosine: a powerful Z-DNA stabilizer. *J. Am. Chem. Soc.*, **125**, 13519–13524.
25. Kohda,K., Tsunomoto,H., Minoura,Y., Tanabe,K. and Shibutani,S. (1996) Synthesis, miscoding specificity, and thermodynamic stability of oligodeoxynucleotide containing 8-methyl-2'-deoxyguanosine. *Chem. Res. Toxicol.*, **9**, 1278–1284.
26. Dalvit,C. (1998) Efficient multiple-solvent suppression for the study of the interactions of organic solvents with biomolecules. *J. Biomol. NMR*, **11**, 437–444.
27. Jeener,J., Meier,B., Bachmann,H.P. and Ernst,R.R. (1979) Investigation of exchange processes by two-dimensional NMR spectroscopy. *J. Chem. Phys.*, **71**, 4546–4553.
28. Braunschweiler,L. and Ernst,R.R. (1983) Coherence transfer by isotropic mixing: application to proton correlation spectroscopy. *J. Magn. Reson.*, **53**, 521–528.
29. Marion,D., Ikura,M., Tschudin,R. and Bax,A. (1989) Rapid recording of 2D NMR spectra without phase cycling. Application to the study of hydrogen exchange in proteins. *J. Magn. Reson.*, **85**, 393–399.
30. Cornell,W.D., Cieplack,P., Bayly,C.I., Gould,I.R., Merz,K.M., Ferguson,D.M., Spellmeyer,D.C., Fox,T., Caldwell,J.W. and Kollman,P.A. (1995) A second generation force field for the simulation of proteins, nucleic acids, and organic molecules. *J. Am. Chem. Soc.*, **117**, 5179–5197.
31. Weiner,S.J., Kollman,P.A., Case,D.A., Singh,U.C., Ghio,C., Alagona,G., Profeta,S. and Weiner,P.J. (1984) A new force field for molecular mechanical simulation of nucleic acids and proteins. *J. Am. Chem. Soc.*, **106**, 765–784.
32. Feigon,J., Koshlap,K.M. and Smith,F.W. (1995) 1H NMR spectroscopy of DNA triplexes and quadruplexes. *Meth. Enzymol.*, **261**, 225–255.
33. Virgilio,A., Esposito,V., Randazzo,A., Mayol,L. and Galeone,A. (2005) 8-Methyl-2′-deoxyguanosine incorporation into parallel DNA quadruplex structures. *Nucleic Acids Res.*, **33**, 6188–6195.
34. Thao Tran,P.L., Virgilio,A., Esposito,V., Citarella,G., Mergny,J.-L. and Galeone,A. (2011) Effects of 8-methylguanine on structure, stability and kinetics of formation of tetramolecular quadruplexes. *Biochimie*, **93**, 399–408.
35. Smith,F.W. and Feigon,J. (1992) Quadruplex structure of *Oxytricha* telomeric DNA oligonucleotides. *Nature*, **356**, 164–167.
36. Sugiyama,H., Kawai,K., Matsunaga,A., Fujimoto,K., Saito,I., Robinson,H. and Wang,A.H.-J. (1996) Synthesis, structure and thermodynamic properties of 8-methylguanine-containing oligonucleotides: Z-DNA under physiological salt conditions. *Nucleic Acids Res.*, **24**, 1272–1278.
37. Esposito,V., Galeone,A., Mayol,L., Oliviero,G., Virgilio,A. and Randazzo,L. (2007) A Topological Classification of G-Quadruplex Structures. *Nucleosides, Nucleotides Nucleic Acids*, **26**, 1155–1159.
38. Masiero,S., Trotta,R., Pieraccini,S., De Tito,S., Perone,R., Randazzo,A. and Spada,G.P. (2010) A non-empirical chromophoric interpretation of CD spectra of DNA G-quadruplex structures. *Org. Biomol. Chem.*, **8**, 2683–2692.
39. Esposito,V., Randazzo,A., Piccialli,G., Petraccone,L., Giancola,C. and Mayol,L. (2004) Effects of an 8-bromodeoxyguanosine incorporation on the parallel quadruplex structure $[d(TGGGT)]_4$. *Org. Biomol. Chem.*, **2**, 313–318.
40. Scaria,P.C., Shire,S.J. and Shafer,R.H. (1992) Quadruplex structure of d($G_3T_4G_3$) stabilized by potassium or sodium is an asymmetric hairpin dimer. *Proc. Natl Acad. Sci. USA*, **89**, 10336–10340.
41. Smith,F.W., Lau,F.W. and Feigon,J. (1994) d($G_3T_4G_3$) forms an asymmetric diagonally looped dimeric quadruplex with guanosine 5′-syn-syn-anti and 5′-syn-anti-anti N-glycosidic conformations. *Proc. Natl Acad. Sci. USA*, **91**, 10546–10550.
42. Keniry,M.A., Strahan,G.D., Owen,E.A. and Shafer,R.H. (1995) Solution structure of the Na^+ form of the dimeric guanine quadruplex $[d(G_3T_4G_3)]_2$. *Eur. J. Biochem.*, **233**, 631–643.
43. Kypr,J., Kejnovska,I., Renciuk,D. and Vorlickova,M. (2009) Circular dichroism and conformational polymorphism of DNA. *Nucleic Acids Res.*, **37**, 1713–1725.
44. Petraccone,L., Erra,E., Esposito,V., Randazzo,A., Mayol,L., Nasti,L., Barone,G. and Giancola,C. (2004) Stability and structure of telomeric DNA sequences forming quadruplexes containing four G-tetrads with different topological arrangements. *Biochemistry*, **43**, 4877–4884.
45. Esposito,V., Virgilio,A., Randazzo,A., Galeone,A. and Mayol,L. (2005) A new class of DNA quadruplexes formed by oligodeoxyribonucleotides containing a 3′-3′ or 5′-5′ inversion of polarity site. *Chem. Commun.*, **31**, 3953–3955.
46. Mergny,J.L., De Cian,A., Ghelab,A., Sacca',B. and Lacroix,L. (2005) Kinetics of tetramolecular quadruplexes. *Nucleic Acids Res.*, **33**, 81–94.
47. Smith,F.W. and Feigon,J. (1993) Strand orientation in the DNA quadruplex formed from the *Oxytricha* telomere repeat oligonucleotide d($G_4T_4G_4$) in solution. *Biochemistry*, **32**, 8682–8692.
48. Dias,E., Battiste,J.L. and Williamson,J.R. (1994) Chemical probe for glycosidic conformation in telomeric DNAs. *J. Am. Chem. Soc.*, **116**, 4479–4480.
49. Gros,J., Rosu,F., Amrane,S., De Cian,A., Gabelica,V., Lacroix,L. and Mergny,J.-L. (2007) Guanines are a quartet's best friend: impact of base substitutions on the kinetics and stability of tetramolecular quadruplexes. *Nucleic Acids Res.*, **35**, 3064–3075.
50. Gros,J., Avino,A., Lopez de la Osa,J., Gonzalez,C., Lacroix,L., Perez,A., Orozco,M., Eritja,R. and Mergny,J.-L. (2008) 8-Amino guanine accelerates tetramolecular G-quadruplex formation. *Chem. Commun.*, **25**, 2926–2928.
51. Petraccone,L., Duro,I., Randazzo,A., Virno,A., Mayol,L. and Giancola,C. (2007) Biophysical Properties of Quadruplexes Containing Two or Three 8-Bromodeoxyguanosine Residues. *Nucleosides, Nucleotides Nucleic Acids*, **26**, 669–674.
52. Cang,X., Sponer,J. and Cheatham,T.E. III (2011) Explaining the varied glycosidic conformational, G-tract length and sequence preferences for anti-parallel G-quadruplexes. *Nucleic Acids Res.*, **39**, 4499–4512.
53. Phan,A.T., Modi,Y.S. and Patel,D.J. (2004) Two-repeat *Tetrahymena* Telomeric d(TGGGGTTGGGGT) Sequence

Interconverts Between Asymmetric Dimeric G-quadruplexes in Solution. *J. Mol. Biol.*, **338**, 93–102.
54. Wang,K.Y., McCurdy,S., Shea,R.G., Swaminathan,S. and Bolton,P.H. (1993) A DNA aptamer which binds to and inhibits thrombin exhibits a new structural motif for DNA. *Biochemistry*, **32**, 1899–1904.
55. Amrane,S., Ang,R.W., Tan,Z.M., Li,C., Lim,J.K., Lim,J.M., Lim,K.W. and Phan,A.T. (2009) A novel chair-type G-quadruplex formed by a *Bombyx mori* telomeric sequence. *Nucleic Acids Res.*, **37**, 931–938.
56. Lim,K.W., Amrane,S., Bouaziz,S., Xu,W., Mu,Y., Patel,D.J., Luu,K.N. and Phan,A.T. (2009) Structure of the human telomere in K^+ solution: a stable basket-type G-quadruplex with only two G-tetrad layers. *J. Am. Chem. Soc.*, **131**, 4301–4309.
57. Phan,A.T. and Patel,D.J. (2003) Two-repeat human telomeric d(TAGGGTTAGGGT) sequence forms interconverting parallel and antiparallel G-quadruplexes in solution: distinct topologies, thermodynamic properties, and folding / unfolding kinetics. *J. Am. Chem. Soc.*, **125**, 15021–15027.
58. Zhang,N., Phan,A.T. and Patel,D.J. (2005) (3+1) assembly of three human telomeric repeats into an asymmetric dimeric G-quadruplex. *J. Am. Chem. Soc.*, **127**, 17277–17285.
59. Xu,Y., Noguchi,Y. and Sugiyama,H. (2006) The new models of the human telomere d[AGGG(TTAGGG)$_3$] in K^+ solution. *Bioorg. Med. Chem.*, **14**, 5584–5591.
60. Ambrus,A., Chen,D., Dai,J., Bialis,T., Jones,R.A. and Yang,D. (2006) Human telomeric sequence forms a hybrid type intramolecular G-quadruplex structure with mixed parallel/ antiparallel strands in potassium solution. *Nucleic Acids Res.*, **34**, 2723–2735.
61. Phan,A.T., Luu,K.N. and Patel,D.J. (2006) Different loop arrangements of intramolecular human telomeric (3+1) G-quadruplexes in K^+ solution. *Nucleic Acids Res.*, **34**, 5715–5719.
62. Luu,K.N., Phan,A.T., Kuryavyi,V., Lacroix,L. and Patel,D.J. (2006) Structure of the human telomere in K+ solution: an intramolecular (3+1) G-quadruplex scaffold. *J. Am. Chem. Soc.*, **128**, 9963–9970.
63. Dai,J., Punchihewa,C., Ambrus,A., Chen,D., Jones,R.A. and Yang,D. (2007) Structure of the intramolecular human telomeric G-quadruplex in potassium solution: a novel adenine triple formation. *Nucleic Acids Res.*, **35**, 2240–2250.
64. Dai,J., Carver,M., Punchihewa,C., Jones,R.A. and Yang,D. (2007) Structure of the Hybrid-2 type intramolecular human telomeric G-quadruplex in K^+ solution: insights into structure polymorphism of the human telomeric sequence. *Nucleic Acids Res.*, **35**, 4927–4940.
65. Phan,A.T., Kuryavyi,V., Luu,K.N. and Patel,D.J. (2007) Structure of two intramolecular G-quadruplexes formed by natural human telomere sequences in K^+ solution. *Nucleic Acids Res.*, **35**, 6517–6525.
66. Webba da Silva,M., Trajkovski,M., Sannohe,Y., Ma'ani,H.N., Sugiyama,H. and Plavec,J. (2009) Design of a G-quadruplex topology through glycosidic bond angles *Angew. Chem., Int. Ed.*, **48**, 9167–9170.
67. Kaushik,M., Bansal,A., Saxena,S. and Kukreti,S. (2007) Possibility of an antiparallel (tetramer) quadruplex exhibited by the double repeat of the human telomere. *Biochemistry*, **46**, 7119–7131.
68. Wyatt,J.R., Vickers,T.A., Roberson,J.L., Buckheit,R.W. Jr, Klimkait,T., DeBaets,E., Davis,P.W., Rayner,B., Imbach,J.L. *et al.* (1994) Combinatorially selected guanosine-quartet structure is a potent inhibitor of human immunodeficiency virus envelope-mediated cell fusion, *Proc. Natl Acad. Sci. USA*, **91**, 1356–1360.
69. Martino,L., Virno,A., Pagano,B., Virgilio,A., Di Micco,S., Galeone,A., Giancola,C., Bifulco,G., Mayol,L. and Randazzo,A. (2007) Structural and thermodynamic studies of the interaction of distamycin a with the parallel quadruplex structure [d(TGGG GT)]$_4$. *J. Am. Chem. Soc.*, **129**, 16048–16056.